Proceedings of the XVIII ECSMGE 2024
GEOTECHNICAL ENGINEERING CHALLENGES
TO MEET CURRENT AND EMERGING NEEDS OF SOCIETY

ISBN 978-1-032-54816-6
DOI 10.1201/9781003431749-81

A closed-form equation for the failure locus of pile groups subjected to generalized loading conditions

Une équation de forme fermée pour le lieu de rupture de groupes de pieux soumis à des conditions de chargement généralisées

M. Iovino*
University of Napoli 'Parthenope', Naples, Italy

C. Iodice, R. Di Laora
University of Campania 'Luigi Vanvitelli', Aversa, Italy

L. de Sanctis
University of Napoli 'Parthenope', Naples, Italy

A. Mandolini
University of Campania 'Luigi Vanvitelli', Aversa, Italy

**maria.iovino@assegnista.uniparthenope.it*

ABSTRACT: A closed-form solution for the failure locus of piled foundations in the force space is presented and discussed. Based on recent works published in the literature dealing with the problem of the bearing capacity of pile groups under inclined eccentric load, the expression of the failure locus is derived by combining a parabola in the vertical force – moment plane and a Granville egg in the vertical force – horizontal force plane. The complete three-dimensional failure surface requires only a few parameters that can be evaluated even by hand calculation through simplified methods existing in literature. The predictive ability of the proposed equation is validated against the data available from previous works on piled foundations subjected to inclined eccentric loads.

RÉSUMÉ: Une nouvelle solution de forme fermée pour le lieu de rupture des fondations sur pieux dans l'espace des forces est présentée et discutée. Basé sur des travaux récents publiés dans la littérature traitant du problème de la capacité portante des groupes de pieux sous charge excentrique inclinée, l'expression du lieu de rupture est dérivée en combinant une parabole dans le plan force verticale – moment et un œuf de Granville dans le plan force verticale – force horizontal. La surface de rupture tridimensionnelle complète ne nécessite que quelques paramètres qui peuvent être évalués même par calcul manuel grâce à des méthodes simplifiées existant dans la littérature. La capacité prédictive de l'équation proposée est validée par rapport aux données disponibles dans de travaux antérieurs sur des fondations sur pieux soumises à des charges excentriques inclinées.

Keywords: Pile group, bering capacity, failure locus, inclined eccentric loads.

1 INTRODUCTION

The evaluation of the pile group bearing capacity under vertical, Q, horizontal, H, and moment, M, loads can be conveniently carried out employing simple solutions as alternative tools to more complex and time-consuming numerical analyses. In this context, interaction domains can be used in engineering practice for a quick and reliable evaluation of the foundation resistance necessary to fulfil design Ultimate Limit State, ULS, checks.

An exact solution for vertical eccentric load has been proposed by Di Laora et al. (2019) using the theorems of limit analysis; this solution is based on the hypotheses of rigid-plastic behaviour of individual piles whose hinged heads are connected through a rigid cap of infinite strength. In the same fashion, to consider general loading conditions, Iovino et al. (2021) and Di Laora et al. (2022) furnished solutions for pile groups under inclined eccentric load postulating the formation of a double plastic hinge at failure to describe the response of the group to the horizontal component (Broms 1964 a, b).

Based on the above works, a closed-form solution for the failure locus of pile groups is derived. In particular, the three-dimentional domain is a combination of a parabola approximating the shape of the interaction diagram in the axial load – moment plane (Di Laora et al., 2019) and a Granville egg to replicate the shape of the surfaces in planes parallel to the axial load – horizontal load plane (Iovino et al. 2021; Di Laora et al. 2022). The use of the proposed domain is straightforward since the constants needed are already required in routine design.

In the following sections the mathematical formulation of the failure locus is presented and a discussion about the selection of the ingredients needed for its construction is provided. Finally, the ability of the proposed expression to match the failure surface of pile groups is demonstrated by comparison with data borrowed from a recent numerical work on pile groups subjected to combined loads.

2 FORMULATION OF THE FAILURE LOCUS

For the sake of simplicity, the formulation of the failure locus is herein shown for the case of a row of four equally-spaced, identical piles. Dealing with the (Q, M) and (Q, H) planes separately, the final three-dimensional expression is presented as a combination of the two.

In Figure 1 a plot of the domain for vertical eccentric load is presented employing the closed-form solution by Di Laora et al. (2019), whose boundary can be reasonably approximated with a parabola passing through the points:

1. (Q_c, 0), where Q_c is the bearing capacity of the pile group in compression;
2. (Q_t, 0), where Q_t is the bearing capacity of the pile group in uplift;
3. ((Q_c+Q_t)/2, M_{max}), where M_{max} is the maximum moment capacity of the pile group.

By imposing such conditions, the following equation is obtained:

$$\left|\frac{M}{M_{max}}\right| = 4\,\frac{(Q_c-Q)(Q-Q_t)}{(Q_c-Q_t)^2} \tag{1}$$

Any section of the failure locus in planes parallel to (Q, H) can be obtained using a trapezium (Figure 2a) whose inclined side connects the points of coordinates (Q_c, H_c) and (Q_t, H_t), where H_c and H_t are the horizontal capacity of the pile group calculated at Q_c and Q_t, respectively (Di Laora et al., 2022). The equation of the inclined line is therefore:

$$H = H_t + \frac{(H_c-H_t)}{(Q_c-Q_t)}(Q-Q_t) = H_t + i_h(Q-Q_t) \tag{2}$$

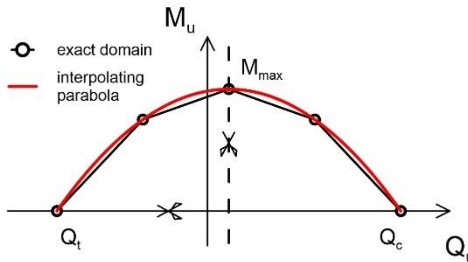

Figure 1. Failure locus for H = 0: exact domain and approximating parabola.

To obtain a smoother shape, the Granville egg was selected and its graphical construction is explained in the following. Consider a circle with centre C and radius r, a point A on the x-axis and a line t parallel to the y-axis (Figure 2b). For any point P with coordinates (x_P, y_P) lying on the circumference, the segment AP intersects line t in point T with coordinates (x_T, y_T). Point Q belonging to the Granville egg has coordinates (x_P, y_T). The whole function is found repeating the above construction for any point of the circumference and can be expressed as:

$$\begin{cases} x_Q = x_p = b + r\cos\omega \\ y_Q = y_T = a\tan\omega = \frac{a\,r\sin\omega}{d+a-r\cos\omega} \end{cases} \tag{3}$$

where b is the abscissa of point C, ω is the central angle defined by points P and A, a is the distance between point A and line t, d is the distance between point C and line t. The Cartesian form may be obtained by manipulating Equations (3) as:

$$y^2 = \frac{a^2[r^2-(x-b)^2]}{[(d+a)-(x-b)]^2} \tag{4}$$

To obtain a good approximation of the failure interaction diagram in the (Q, H) plane for M = 0, the passage through the following points is imposed:

1. (Q_c, 0);
2. (Q_t, 0);
3. point E on the inclined side of the trapezium whose position controls the shape of the egg, with coordinates (Q_E, H_E) = (Q_t + 2βR, H_t + 2$i_h\beta R$), where β is a dimensionless position, and $r = R = (Q_c - Q_t)/2$;

In addition to the above, the following condition is also considered:

4. horizontal tangent at $Q = Q_E$, i.e. $H_E = H_{max}$.

The parameters in Equation (4) can be therefore expressed as:

$$\begin{cases} b = \frac{Q_c+Q_t}{2} \\ r = R = \frac{Q_c-Q_t}{2} \\ a = 2\frac{H_t+2i_h\beta R}{2\beta-1}\sqrt{\beta(1-\beta)} \\ d = \frac{R}{2\beta-1} - a \end{cases} \quad (5)$$

For β it is suggested to take:

$$\begin{cases} \beta = \frac{1+2\psi}{2(1+\psi)} \\ \psi = 1 - \frac{H_t}{H_c} \end{cases} \quad (6)$$

The parameter β varies monotonically within the range [0.5, 0.75]. It is equal to 0.5 when the two lateral capacities are identical and to 0.75 when the failure domain degenerates in a triangle, that is for $H_t = 0$. Also, the Granville egg is defined only for H_c strictly larger than H_t; when H_c tends to H_c the egg approaches an ellipse.

Finally, the equation of the Granville egg for $M = 0$ is:

$$\left(\frac{H}{H_{max}}\right)^2 = \frac{4\beta(1-\beta)\left[\left(\frac{Q-b}{R}\right)^2-1\right]}{\left[(2\beta-1)\left(\frac{Q-b}{R}\right)-1\right]^2} \quad (7)$$

Note that the symmetric portion of the domain in the (Q, M) and (Q, H) planes can be obtained by changing the sign on the right-hand side of Equations (1) and (7), respectively.

To construct the three-dimensional surface starting from the above-defined sections for $H = 0$ and $M = 0$, the following procedure is established.

For any value of $M \neq 0$ it is possible to use Equation (1) to determine the corresponding Q_1 and Q_2 on the parabola as:

$$\begin{cases} Q_1 = \frac{Q_c+Q_t}{2} - R\sqrt{1-\frac{M}{M_{max}}} \\ Q_2 = \frac{Q_c+Q_t}{2} + R\sqrt{1-\frac{M}{M_{max}}} \end{cases} \quad (8)$$

The loads Q_1 and Q_2 can be used in Equation (2) to calculate the interaction domain in the (Q, H) plane for $M \neq 0$:

$$\begin{cases} H_1 = H_t + i_h(Q_1 - Q_t) \\ H_2 = H_t + i_h(Q_2 - Q_t) \end{cases} \quad (9)$$

This failure domain can be still interpolated by the Granville egg using as ultimate loads in Equations (5) and (6) the values calculated through Equations (8) and (9).

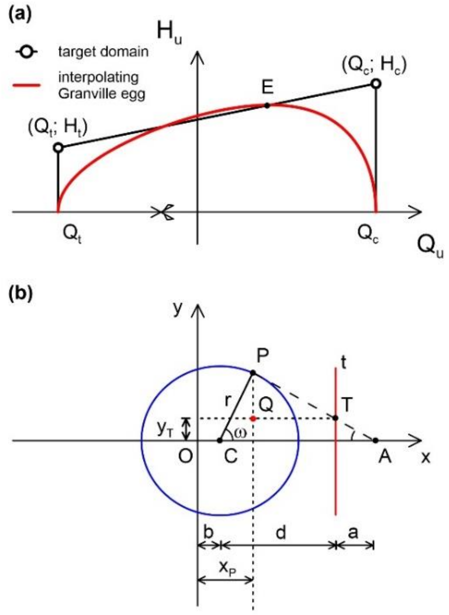

Figure 2. Fitting of Granville's egg to the target domain in the (Q, H) plane (a); graphical example of Granville's egg construction.

Substituting Equation (9) into Equation (7) yields to:

$$f = \left\{H^2\left[R\sqrt{1-\frac{M}{M_{max}}} - (2\beta-1)(Q-b)\right]^2 + \right.$$
$$+ 4\beta(\beta-1)\left[R^2\left(1-\frac{M}{M_{max}}\right) - (Q - b)^2\right]\left[H_{max} + i_h R(2\beta-1)\left(\sqrt{1-\frac{M}{M_{max}}} - 1\right)\right]^2\left.\right\}/(2\beta-1)^2 = 0 \quad (10)$$

which is the explicit expression of the 3D failure locus (Figure 3).

Equation (10) is completely defined by only 5 parameters, (Q_c, Q_t, H_c, H_t, M_{max}) which can be determined even by hand calculation. In particular, Q_c and Q_t can be easily derived from the axial capacities in compression (N_u) and uplift ($-S_u$) of the isolated pile employing one of the possible approaches available in literature (e.g., Fleming et al, 2008; Letizia et al., 2018) and considering the efficiency at failure (e.g., Vesic, 1969; De Mello, 1969); M_{max} is evaluated form Q_c and Q_t using the approach proposed by Di Laora et al. (2019); H_c and H_t can be calculated from the horizontal capacities of the isolated pile subjected to an axial load equal to N_u and $-S_u$, respectively, as shown by Iovino et al. (2021) and Di Laora et al. (2022).

It is worth mentioning that Equation (10) can be conveniently used in routine engineering for ULS checks of pile foundations when subjected to the contemporary presence of three load components or incorporated in more complex mathematical frameworks, such as macroelements, serving as failure surface for the evaluation of the foundation response (Iodice et al., 2023, 2024).

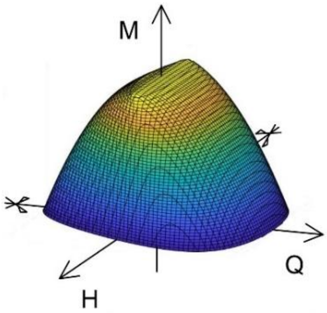

Figure 3. 3D failure surface.

3 VALIDATION AGAINST NUMERICAL ANALYSES

To show the predictive capabilities of the proposed failure surface, the latter is compared to the results of the Finite Element analyses available in literature on small pile groups subjected to an inclined eccentric load by Psychari & Anastasopoulos (2022). The Authors performed a series of analyses on (2 × 1), (3 × 1) and (4 × 1) pile groups. In the following only the comparison with the (2 × 1) group is presented since the results at failure are available for all the load components solely for this case.

The FE analysis involve a load path with an initial branch in which the group is only loaded vertically; after that, the horizontal load is applied under constant eccentricity represented by the pier height, h_{pier} = 6 m or 20 m. An idealized, homogeneous clay deposit with uniform undrained shear strength s_u = 100 kPa is considered. The soil behaviour is modelled with a kinematic hardening model with von Mises failure criterion and associated flow rule, while Reinforced Concrete (RC) piles are idealized by a combination of non-linear continuum elements for the concrete and surface elements for the longitudinal reinforcement so as to simulate the dependence of the plastic yielding moment of the pile cross-section, M_y, from the axial load, N. To investigate in detail the mechanism of interaction under combined loads, Psychari & Anastasopoulos (2022) distinguish between the moment component due to the axial resistance of the piles and that associated to the flexural strength of the concrete cross-section, referred to in the original work as M_{ax} and M_b, respectively. Since in the present formulation M_b is neglected, the focus is set only on the first contribution, M_{ax}.

The 5 parameters to employ in Equation (10) are derived as detailed in the ensuing and summarized in Table 1. The axial capacities in compression, Q_c, and tension, Q_t, of each pile group are evaluated from the axial capacities of the isolated pile, N_u and ($-S_u$), determined by employing analytical solutions. An efficiency factor of unity is adopted in this case. The moment capacity of the group, M_{max}, is calculated from N_u and ($-S_u$), using the solution by Di Laora et al. (2019). Considering the layout of the longitudinal reinforcement and the material properties of the RC piles, the horizontal capacities of the single pile are first estimated applying the Broms (1964a) theory for fixed head piles in clay with a yielding moment calculated by the closed-form expression proposed by Di Laora et al. (2020) under an axial force equal to N_u or ($-S_u$); then, the horizontal capacities of the group, H_c, and H_t, are obtained postulating an efficiency factor under horizontal load equal to unity.

Table 1. Parameters of the failure surface adopted to reproduce the analyses by Psychari & Anastasopoulos (2022) for (2 × 1) pile group.

Q_c (MN)	Q_t (MN)	M_{max} (MNm)	H_c (MN)	H_t (MN)
8.48	-7.07	11.66	4.15	0.15

The results of the comparison are shown in Figure 4 for the two cases of h_{pier} = 6 m and 20 m. The sections of the interaction domains in the (Q, M) plane are reported for H = 0 and $H = H_f$, H_f being the horizontal failure load at the end of the applied multicomponent load path as derived from the proposed failure locus; likewise, the sections in the (Q, H) plane are plotted for M = 0 and $M = M_f$, M_f being the moment at failure for the applied multicomponent load path as derived from the proposed failure locus. Note that since the vertical load is very small (10% of the group vertical bearing capacity) and $M_f \approx M_{max}$, the three-dimensional shape of the failure locus is such that the sections for $M = M_f$ in the (Q, H) plane are very narrow (a zoom is provided in the rightmost side of the figure). It can be stated that Equation (10) matches in a satisfactory way the data from FE analyses. The difference in the previsions (e.g., M_f = 0.85 and 0.9 M_{FE}, for h_{pier} = 6 m and 20 m, respectively, M_{FE} is the moment derived from FE analyses) can be explained inspecting the moment – rotation and horizontal load–horizontal displacement curves by Psychari & Anastasopoulos (2022), not reported here for space limitations. Note that the proposed failure locus is inherently not able to replicate the hardening response as predicted by the FE model at very large rotations.

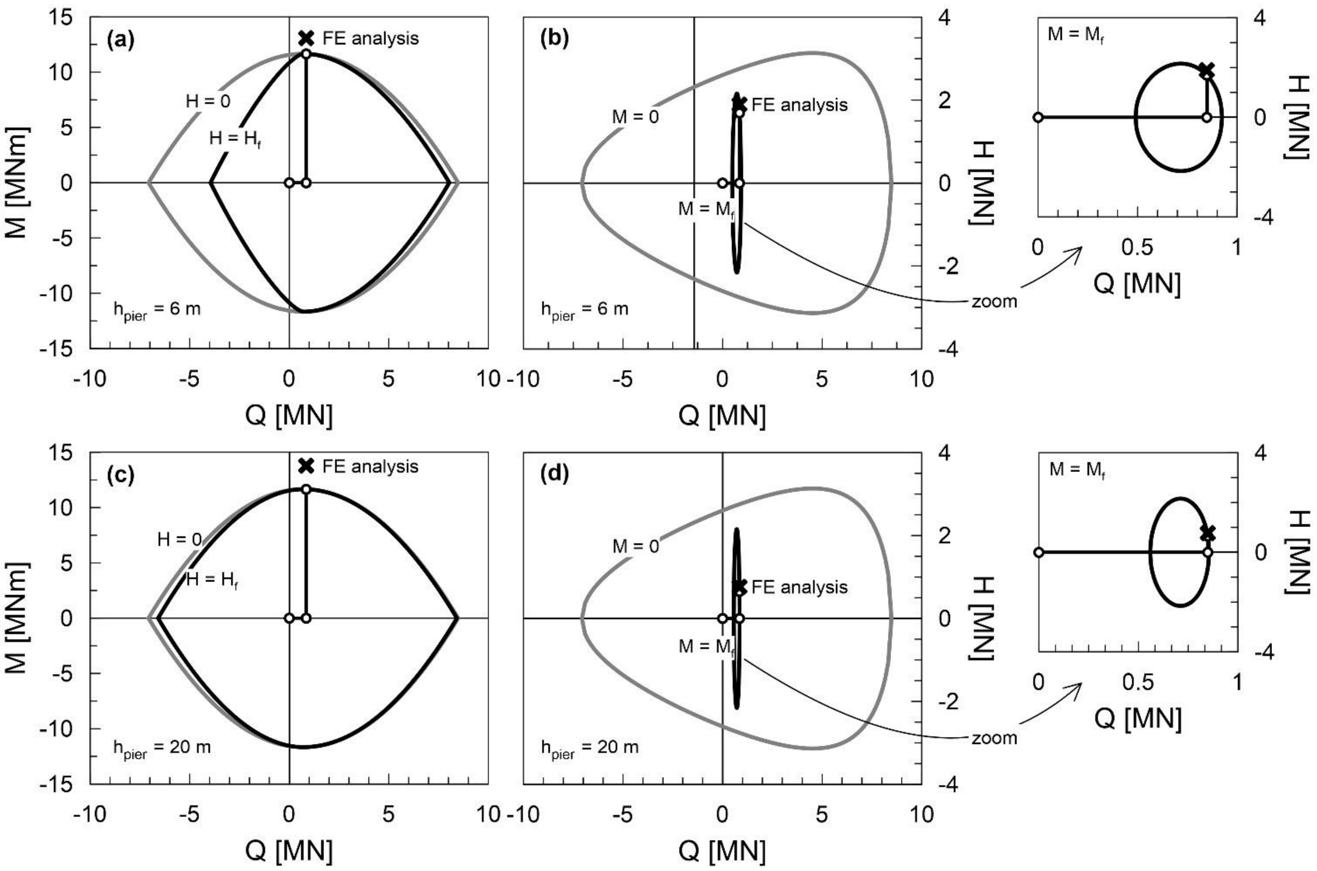

Figure 4. Comparison between Equation (10) and the FE analyses by Psycari and Anastasopoulos (2022).

4 CONCLUSIONS

The work describes a closed form equation for the evaluation of the failure locus of a pile group subjected to a multicomponent load including vertical, horizontal and moment components. The three-dimensional locus is obtained as a combination of a parabola and the Granville egg. In particular, the parabola is used to approximate the shape of the interaction diagram in the axial load–moment plane, while the Granville egg is employed to replicate the shape of the surfaces in planes parallel to the axial load–horizontal load plane. The use of the proposed failure domain is straightforward since the parameters needed for its construction are simple to determine even with hand calculations and anyhow are already required in routine design.

The ability of the failure locus in predicting the behaviour of pile groups subjected to vertical eccentric load has been checked against data from rigorous numerical analyses on small pile groups available in literature, providing generally good performance.

The proposed closed form equation can be conveniently employed for ULS analysis and design of a pile group when subjected to multicomponent loads; in addition, it may serve as an ingredient of more complex mathematical approaches (e.g., macroelements) to derive the load-displacement response of the group under generalized load paths.

ACKNOWLEDGEMENTS

The authors are grateful for the financial support provided by the Italian Ministry for Research and University. The project presented in this article is supported by MIUR PRIN 2017 ‘A new macro-element model for pile groups under monotonic, cyclic and dynamic loadings’.

REFERENCES

Broms, B.B. (1964a) Lateral resistance of piles in cohesive soils. *Journal of Soil Mechanics Foundation Division* 90(2):27–63. https://doi.org/10.1061/JSFEAQ.0000611.

Broms, B.B. (1964b) Lateral resistance of piles in cohesionless soils. *Journal of Soil Mechanics Foundation Division* 90(3):123–156. https:doi.org/10.1061/JSFEAQ.0000614.

De Mello, V. F. B. (1969). Foundations of Buildings on Clay. In State of the Art Report, *Proceedings of the 7th International Congress on Soil Mechanics and Foundation Engineering*, Vol. 1, pp. 49-136.

Di Laora, R., de Sanctis L., Aversa S. (2019). Bearing capacity of pile groups under vertical eccentric load. *Acta Geotechnica*. 14 (1), 193–205. https://doi.org/10.1007/s11440-018-0646-5.

Di Laora, R., Galasso, C., Mylonakis, G., Cosenza, E. (2020). A simple method for N-M interaction diagrams of circular reinforced concrete cross sections. *Structural Concrete*, 21(1), 48-55. https://doi.org/10.1002/suco.201900139.

Di Laora, R., Iodice, C., Mandolini, A. (2022). A closed-form solution for the failure interaction diagrams of pile groups subjected to inclined eccentric load. *Acta Geotechnica*, 17(8), 3633-3646. https://doi.org/10.1007/s11440-021-01439-8.

Fleming K.,Weltman, A., Randolph, M., Elson, K. (2008). *Piling engineering*. CRC Press. https://doi.org/10.1201/b22272.

Iodice, C., Iovino, M., Di Laora, R., de Sanctis, L., Mandolini, A. (2023). A Macro-element for Pile Groups Subjected to Vertical Eccentric Load. In *Proceedings of the National Conference of the Researchers of Geotechnical Engineering*, Cham: Springer Nature Switzerland, pp. 201-217. https://doi.org/10.1007/978-3-031-34761-0_26.

Iodice, C., Iovino, M., Di Laora, R., de Sanctis, L., Mandolini, A. (2024). A strain-hardening macro-element model for pile groups under vertical-horizontal-moment loading. *Acta Geotechnica*, 1-15. https://doi.org/10.1007/s11440-023-02174-y.

Iovino, M., de Sanctis, L., Maiorano, R.M.S., Aversa, S. (2021). Failure envelopes of pile groups under inclined eccentric load. *Géotechnique Letters*, 11(4), 247-253. https://doi.org/10.1680/jgele.21.00059.

Letizia, N., Iodice, C., Mandolini, A. (2018). A local design method for pile foundations. *Advances in Civil Engineering*. https://doi.org/10.1155/2018/9486945.

Psychari, A., Anastasopoulos, I. (2022). Combined loading of RC pile groups in clay accounting for N–M interaction. *Soil Dynamics and Earthquake Engineering*, 163, 107490. https://doi.org/10.1016/j.soildyn.2022.107490.

Vesić, A. (1969). Experiments with instrumented pile groups in sand. In *Performance of deep foundations*. ASTM International. https://doi.org/10.1520/STP47286S.